Synthesis of Comblike Poly(styrene-*b*-isoprene) Block Copolymers and Their Properties in Good and Selective Solvents

David Lanson, Michel Schappacher, Alain Deffieux,* and Redouane Borsali*

Laboratoire de Chimie Organiques des Polymères Organiques, LCPO, CNRS, ENSCPB, and Bordeaux 1 University, 16 Avenue Pey Berland, 33607 PESSAC Cedex, France

Received May 24, 2006; Revised Manuscript Received July 27, 2006

ABSTRACT: Comblike block copolymers having a poly(chloroethyl vinyl ether) backbone and poly(styrene-*b*-isoprene) side chains, i.e., PCEVE-*g*-(PS-*b*-PI), of different molar masses and chemical compositions were synthesized by "grafting onto" technique using the coupling reaction of acetal−PSLi (F−PSLi) chains onto the reactive functions of a PCEVE backbone, followed, in a second step, by the grafting of living PIDLi chains onto the acetal ends of PS branches activated by trimethyl silyl iodide. The comblike copolymers exhibit low polydispersity, high molar masses, and a controlled number of branches. Their characteristics and behavior were further studied in the solid as thin films and in good and selective solvents. Atomic force microscopy (AFM) shows isolated uniform molecules that adopt an ovoid conformation. The solution behavior of these comblike polymers was investigated by dynamic light scattering (DLS), both in a good solvent of the PS and the PI blocks and in selective solvents of the outer PI blocks. Depending on the solvent quality and the temperature, the comblike copolymers, which remain in the form of isolated molecules, adopt different chain conformations and dimensions, as shown by the drastic variation of the radius of gyration. In a series of hydrocarbon solvents of decreasing quality for the inner PS block, the significant volume decrease of the macromolecule is attributed to the internal shrinkage of the PS blocks. In cyclohexane, a θ solvent for the inner PS block, a strong variation of the comblike size (90% volume change) takes place with the temperature change, directly correlated with the internal expansion/contraction of the inner PS blocks.

1. Introduction

Besides other key parameters such as chemical composition, comonomer unit distribution, molar masses, polydispersity, etc., chain architecture can play an important role in the design of specific properties of macromolecules. For example, very different behaviors in the mode of organization and assembly of linear and highly branched polymers and copolymers have been reported both in solution and in the bulk.[1−5] This important role of chain topology on the properties has led to an increasing interest in the preparation and study of polymers with branched and hyperbranched chain architectures. Among this category, comblike polymers and copolymers represent an important and easily accessible class of materials.[6−13]

In the present work, we have prepared a series of comblike copolymers with diblock branches, i.e., polychloroethyl vinyl ether-*g*-(polystyrene-*b*-polyisoprene), PCEVE-*g*-(PS-*b*-PI). These multibranched macromolecules can be visualized as potentially persistent unimolecular micelles constituted by the assembly of elementary PS-*b*-PI block copolymers, (the branches) covalently attached by the free extremity of the PS block to the core center, the PCEVE backbone. The solution properties of these diblock comblike copolymers and their potential behavior as unimolecular micelles was investigated in various solvents, either good for the PS and PI blocks or selective of the PI blocks (outer block).

2. Experimental Section

2.1. Materials. Cyclohexane and toluene (99.5%, J. T. Baker, Deventer, The Netherlands) were purified by distillation over calcium hydride and stored over polystyryllithium seeds. α-Chloroethyl vinyl ether (CEVE) (99%, Sigma-Aldrich Chimie, Saint Quentin Fallavier, France) was washed with an aqueous NaOH solution (1 N) and distilled twice over calcium hydride. Styrene and Isoprene (99%, Sigma-Aldrich Chimie, Saint Quentin Fallavier, France) was purified by distillation over calcium hydride at reduced pressure. *N*,*N*,*N*′,*N*′-Tetramethylethylenediamine (TMEDA) (99.5%, Sigma-Aldrich Chimie, Saint Quentin Fallavier, France) was dried and purified by distillation over sodium. *sec*-Butyllithium (1.3 M in cyclohexane, Sigma-Aldrich Chimie, Saint Quentin Fallavier, France) was used as received. All the reactants were stored under dry nitrogen in a glass apparatus fitted with PTFE stopcocks.

2.2. Polymerization Procedures. *2.2.1. Synthesis of the PCEVE Backbone and the PCEVE-g-(PS−F) Comblike Polymers.* The preparation of these polymers has been described in detail in previous contributions.[14] Briefly, a poly(chloroethyl vinyl ether) (PCEVE) (a), $\overline{DP}_{n(PCEVE)} = 230$; $\bar{M}_w/\bar{M}_n = 1.03$, was first synthesized by living cationic polymerization of chloroethyl vinyl ether using propyl diethylacetal/trimethyl silyl iodide as the initiating system and zinc chloride as the catalyst and used as a reactive backbone.[15] Living α-diethylacetal polystyryllithium chains (Scheme 1a) were then prepared using propyllithium diethylacetal as an initiator and grafted onto the PCEVE backbone by adding the living F−PSLi solution onto a known quantity of PCEVE in cyclohexane solution to form a comblike polymer with α-diethylacetal polystyrene branches, (PCEVE-*g*-(PS−F)) (Scheme 1b). Selective precipitation of the polymer solution in heptane allowed recovery of the F−PS comb free of ungrafted linear F−PS.

2.2.2. Synthesis of the PCEVE-g-(PS-b-PI) Comblike Block Copolymers. A typical reaction procedure is described below. PCEVE-*g*-(PS−F) comblike polymers (1′) with $\overline{DP}_{n(PCEVE)} = 230$, $\overline{DP}_{n(PS)} = 122$ (1.6 g, 1.3×10^{-4} mol in PS branch equation) was placed in a 500 mL glass reactor fitted with PTFE stopcocks and dissolved in 20 mL of dry toluene. To remove any traces of moisture from the polymer, the solvent was evaporated under vacuum and replaced by a new volume of dry toluene. The operation was repeated twice. The polymer was then finally redissolved into anhydrous toluene (200 mL). The reactor was thermostated at −30 °C and TMSI (35 μL, 2.6×10^{-4} mol) was added to convert the PS−acetal end groups into iodoether groups (Scheme 1d). After

* Corresponding authors. E-mail: deffieux@enscpb.fr (A.D.); borsali@enscpb.fr (R.B.).

10.1021/ma061169l CCC: $33.50
Published on Web 09/12/2006

Scheme 1

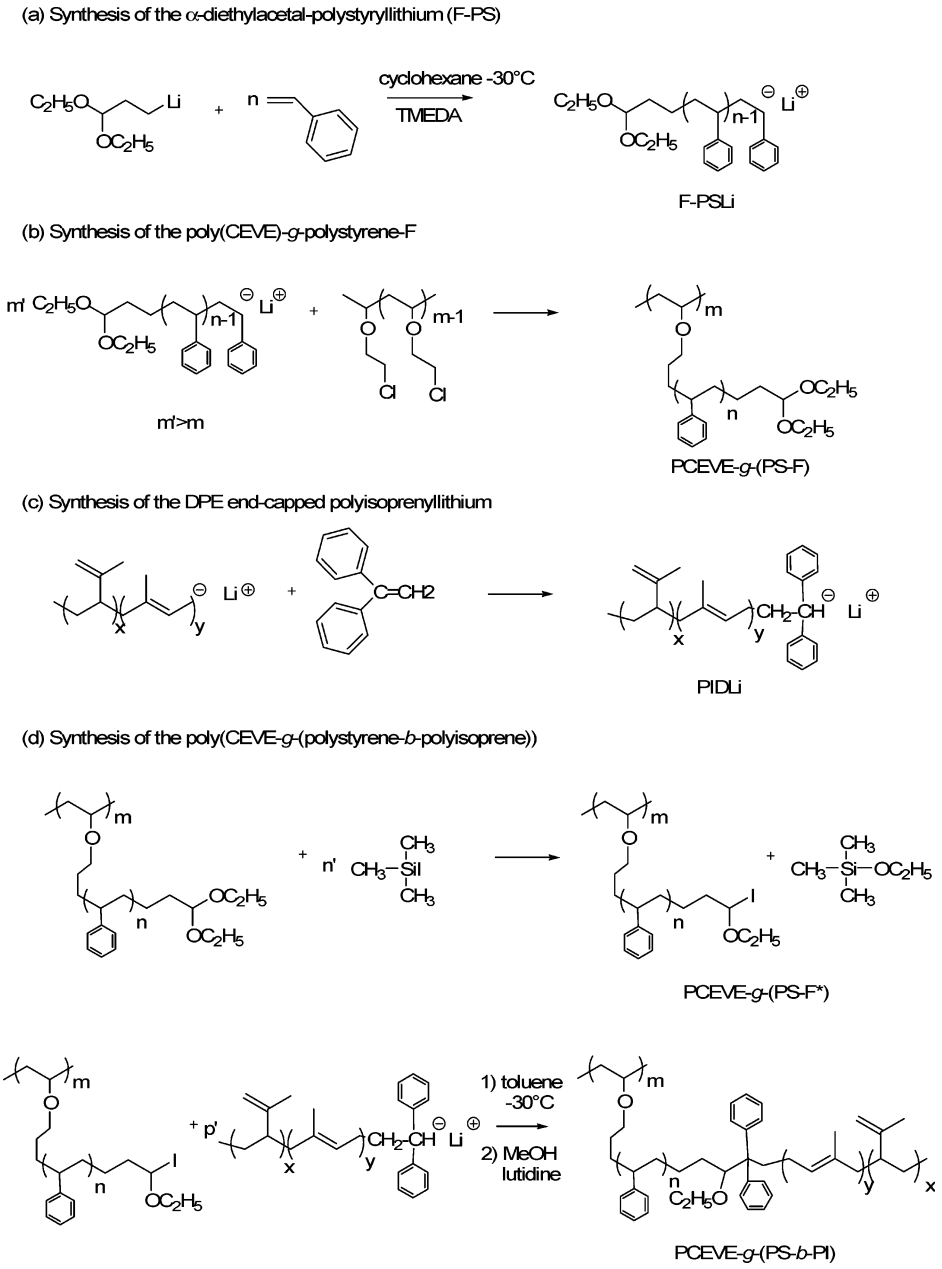

about 30 min stirring at −30 °C, a red solution of polyisoprenyllithium end-capped with one unit of DPE (Scheme 1c), PIDLi, with $\overline{DP}_{n(PI)}$= 78, previously prepared in toluene using *sec*-butyllithium, was then incrementally added to the TMSI-modified PCEVE-*g*-(PS−F). The rate of PIDLi addition was determined by the disappearance of the coloration of the solution, and PIDLi was added until a fading pink color of the reacting media remained over about a 24 h period. At the end of the reaction, a lutidine/methanol (10 mL, 1 mol/L) solution was added to deactivate the polymerization system.

The obtained polymer solution was then washed several times with a solution of potassium thiosulfate (50 mL, 2:100 weight) and neutral water. The excess of PIDLi added was easily removed from the comblike block copolymers by selective precipitation into cyclohexane/acetone (1:4).

3. Analysis and Characterization Techniques

3.1. Static and Dynamic Scattering Measurements. They were performed using the ALV (Langen, FRG) apparatus consisting of an automatic goniometer table, a digital rate meter, and a temperature control of the sample cell within $t \pm 0.1$ °C. The scattered light of a vertically polarized $\lambda_0 = 4880$ Å argon laser (Spectra-Physics 2020, 3 W, operating around 0.3 W) was measured at different angles in the range of 40−150° corresponding to $1.2 \times 10^{-3} < q/\text{Å} < 3.3 \times 10^{-3}$ where $q = (4\pi n/\lambda_0)\sin(\theta/2)$, θ is the scattering angle, and n is the refractive index of the medium ($n = 1.33$). The reduced elastic scattering $I(q)/kC$, with $K = 4\pi^2 n_0 (\mathrm{d}n/\mathrm{d}c)^2 (I_0^{90°}/R^{90°})/\lambda_0^4 N_A$, was measured in steps of 2° in the scattering angle, where n_0 is the refractive index of the standard (toluene), $I_0^{90°}$ and $R^{90°}$ are the intensity and the Rayleigh ratio of the standard at $\theta = 90°$, respectively, dn/dc is the increment of the refractive index, C is the concentration, expressed in g/cm^3, and $I(q)$ is the intensity scattered by the sample. All elastic intensities were calculated according to standard procedures using toluene as the standard with known absolute scattering intensity.

For the dynamic properties, the experiments were carried out in steps of 20° in the scattering angle. The ALV5000 autocorrelator (ALV, FRG) was used to compute the autocorrelation

Table 1. Characteristics of PCEVE-*g*-(PS−F) and PCEVE-*g*-(PS-*b*-PI) Comblike Polymers

ref no.	constitutive blocks $\overline{DP}_n$ PCEVE-PS−PI	$\bar{M}_{w,th}$[a] (g/mol × 10^{-6})	$\bar{M}_{w,exp}$(LS)[b] (g/mol × 10^{-6})	$\bar{M}_w/\bar{M}_n$	grafting efficiency, %[c] PS	PI	$\Phi_{vPS/PI}$[d]
(1)	230−106−0	2.6	2.1	1.06	81	-	100/0
(1′)	230−122−0	2.8	2.4	1.21	87	-	100/0
(2)	230−106−21	2.9	2.3	1.16	81	92	87/13
(2′)	230−122−78	4.2	3.6	1.63	87	94	67/33
(3)	230−106−115	4.4	3.8	1.20	81	97	55/45

[a] Assuming one F−PS block grafted per CEVE unit $\bar{M}_{w,th} = \bar{M}_{w,PCEVE} + 230 \times \bar{M}_{w,F-PS} + 230 \times \bar{M}_{w,PI}$. [b] $\bar{M}_{w,exp}$ determined by light scattering (LS) in THF at 25 °C: $dn/dc = 0.181$ for PCEVE-*g*-(PS−F) and $dn/dc = 0.173, 0.163, 0.129$ for, respectively, PCEVE-*g*-(PS-*b*-PI) (2), (2′), and (3). [c] Coupling efficiency based on the molar mass determined by SLS. [d] $\Phi_{vPS/PI}$ correspond to the volume fractions of PS and PI; the volume of PCEVE (<1%) was neglected.

functions $I(q, t)$ from the scattered intensity data. The autocorrelation functions of the scattered intensity, deduced from the Siegert relation,[16] were analyzed by means of the cumulant method and Contin analysis to give the effective diffusion coefficient $D = \Gamma(q)/q^2$ as a function of the scattering angle and ultimately the hydrodynamic radius $R_H = k_B T/(6\pi\eta D)$, when η is the viscosity of the medium.

3.2. Atomic Force Microscopy (AFM). Samples for AFM analysis were prepared by solvent casting at ambient temperature conditions by spin coating on substrates starting from solutions in dichloromethane. Practically, 20 μL of a dilute solution (0.01 wt %) were spin-cast on a 1 × 1 cm^2 highly oriented pyrolytic graphite (HOPG) substrate. Samples were analyzed after complete evaporation of the solvent at room temperature. All AFM images were recorded in air with a Dimension microscope (Digital Instruments, Santa Barbara, CA), operated in tapping mode. The probes were commercially available silicon tips with a spring constant of 40 N/m, a resonance frequency lying in the 270−320 kHz range, and a radius of curvature in the 10−15 nm range. In this work, both the topography and the phase signal images were recorded with the highest sampling resolution available, i.e., 512 × 512 data points.

3.3. Other Characterization Techniques and Measurements. H^1NMR spectra were recorded in $CDCl_3$ on a Bruker Avance 400 MHz FT apparatus. Size exclusion chromatography (SEC) analysis in THF (distilled from CaH_2) was performed at 25 °C at a flow rate of 0.7 mL/min using a Varian apparatus equipped with refractive index/laser light scattering (Wyatt technology) dual detector and fitted with four TSK columns (300 × 7.7 mm^2, 250, 1500, 10^4, and 10^5 Å, respectively).

4. Results and Discussion

The synthesis of branched polymers has been achieved so far by three main methods often referred as the "grafting from" (grafting side chains from the backbone),[17,18] the "grafting through" (homopolymerization of macromonomers),[1,19] and the "grafting onto" (attachment of side chains to the backbone) approaches.[20,21] The "grafting onto" approach that we have developed in the past years in our group allows the preparation of highly branched macromolecules with long side chains of almost uniform length and with a high backbone grafting density corresponding approximately to 0.8−0.9 branches per backbone unit.[22] This synthetic procedure is based on the selective coupling of living anionic polymer chains of controlled molar mass and low dispersity onto a reactive polymer backbone of controlled dimensions, bearing electrophilic anchoring sites. The latter is prepared by living cationic polymerization of chloroethyl vinyl ether (CEVE).

In this work, we have used a similar procedure to first prepare well-defined comblike polymers polychloroethyl vinyl ether-*g*-(α-diethylacetal polystyrene), (PCEVE-*g*-(PS−F)) of different branch compositions and molar masses. α-diethylacetal−polystyryllithium (F−PSLi) was synthesized by initiation of styrene anionic polymerization from 3-lithiopropyl diethyl acetal in cyclohexane, in the presence of *N*,*N*,*N*′,*N*′-tetramethylethylenediamine (TMEDA). F−PS with $\bar{M}_n$ = 11040 g/mol ($\overline{DP}_{n(PS)}$ = 106) and $\bar{M}_n$ = 12 706 g/mol ($\overline{DP}_{n(PS)}$ = 122), both with $\bar{M}_w/\bar{M}_n$= 1.02, were prepared and grafted onto a PCEVE backbone of $\overline{DP}_n$ = 230. After fractionation using selective precipitation in an cyclohexane/heptane mixture (1:5), the F−PS combs were characterized using proton NMR, size exclusion chromatography (SEC) and light scattering technique. The characteristics of the corresponding PCEVE-*g*-(PS−F) (1) and (1′) are collected Table 1.

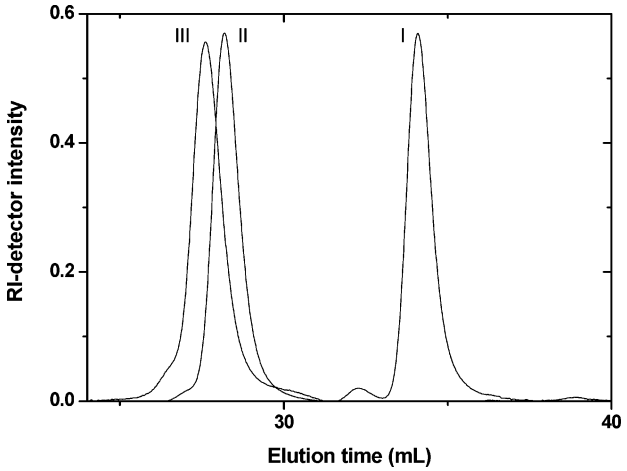

Figure 1. SEC traces recorded at the different building stages of the synthesis of comblike block copolymers: (I) $PCEVE_{230}$ backbone, (II) $PCEVE_{230}$-*g*-PS_{106}−F, and (III) $PCEVE_{230}$-*g*-(PS_{106}-*b*-PI_{21}).

The functional F−PS combs were then used as macromolecular precursors for the preparation of the corresponding comblike PS-*b*-PI diblock copolymers, polychloroethyl vinyl ether-*g*-(polystyrene-*b*-polyisoprene), PCEVE-*g*-(PS-*b*-PI), as indicated in Scheme 1. Several attempts were made to directly graft PI-*b*-PSLi block copolymers onto the PCEVE backbone. Although the grafting efficiency was good, the fractionation between the comb copolymer and ungrafted PS-*b*-PI could not be achieved cleanly due to the formation of PS-*b*-PI micelles. In the present work, the external PI block was introduced in a separate step by a "grafting onto" reaction involving the deactivation of diphenylethylene end-capped living polyisoprene chains (PIDLi, D for DPE) onto the α-iodoether ends of PS branches. The α-iodoether function (F*) was generated in situ by reaction of the PS−acetal end group with trimethyl silyl iodide, Scheme 1, step d. The grafting reaction was then achieved by adding dropwise the red PIDLi solution into a known amount of PCEVE-*g*-(PS−F*) comb. Complete

Table 2. Characteristics and Dimensions in THF at 25 °C of the F−PS Comblike Polymers and the PS-*b*-PI Comblike Block Copolymers

ref no.	constitutive blocks, $\overline{DP}_n$ PCEVE-PS−PI	R_{H0} (nm)[a]	R_{H0} (nm)[b]	R_g (nm)[c]	R_g (nm)[b]	$R_g{}^c/R_{H0}{}^a$ exptl	$R_g{}^b/R_{H0}{}^b$ calcd
(1)	230−106−0	19.4	15.5	24.7	21.6	1.27	1.39
(1′)	230−122−0	19.7	16.2	24.9	22.1	1.26	1.36
(2)	230−106−21	20.6	19.2	21.7	24.4	1.05	1.27
(2′)	230−122−78	23.2	23.1	25.9	27.6	1.12	1.19
(3)	230−106−115	26.3	24.0	29.3	28.3	1.11	1.18

[a] R_{H0} determined using DLS extrapolated to infinite dilution (C → 0). [b] R_{H0} and R_g is deduced from the prolate ellipsoid model. [c] R_g determined using SLS from Zimm method.

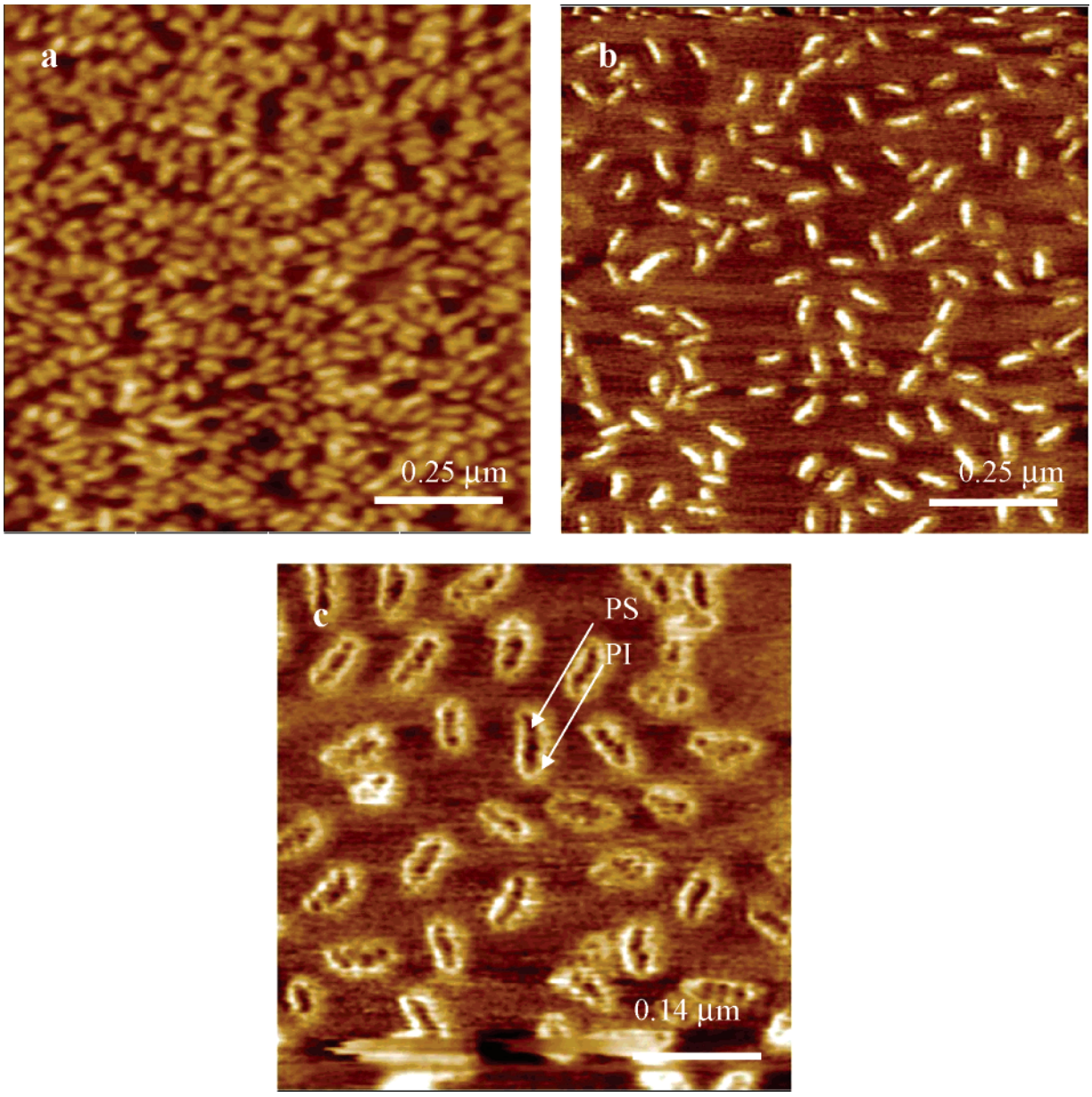

Figure 2. AFM tapping topographic image of (a) $PCEVE_{230}$-*g*-(PS_{106}-*b*-PI_{21}), (b) $PCEVE_{230}$-*g*-(PS_{106}-*b*-PI_{115}) obtained from deposit of methylene dichloride solutions on graphite. Phase image of (c) $PCEVE_{230}$-*g*-(PS_{106}-*b*-PI_{115}), showing the separated hard PS and soft PI phases.

discoloration of the final PIDLi aliquots required several hours. To achieve maximal grafting, PIDLi was added until a persistent light-red coloration of the medium was observed for about 24 h. The excess of PI (D for DPE is omitted in the final PI polymer and copolymer structures) was then removed from the comblike block copolymers by selective precipitation into a cyclohexane/acetone mixture (1:4). The characteristics of the different comblike diblock copolymers (2), (2′), and (3) are given in Table 1.

The theoretical molar masses of the F−PS comb polymers and PS-*b*-PI comb copolymers calculated from the $\overline{DP}_n$ of the PCEVE backbone and that of the F−PS and PI grafts, assuming one graft per CEVE unit, fit very well with experimental molar masses determined using light scattering detection. They correspond to a grafting efficiency between 80 and 90% for the F−PS and close to 100% for the PI blocks. This result suggests that only a few unreacted CEVE units remain in the final

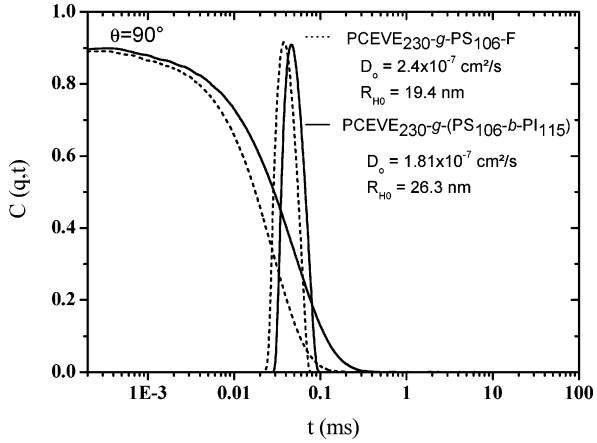

Figure 3. Normalized field correlation and corresponding relaxation times at $\theta = 90°$ for a concentration of 2.2 g/L solution in THF at the temperature of 25 °C for: (a) PCEVE$_{230}$-*g*-PS$_{106}$−F and (b) PCEVE$_{230}$-*g*-(PS$_{106}$-*b*-PI$_{115}$).

comblike PS-*b*-PI block copolymer and that almost all the F−PS are linked to a PI block. Typical SEC chromatograms of a PCEVE polymer and of the corresponding PCEVE-*g*-(PS−F) and PCEVE-*g*-(PS-*b*-PI) combs are shown in Figure 1.

4.1. AFM Imaging. To further characterize the architectural parameters of the comb copolymers, their conformation was investigated by AFM. Highly diluted solutions of the copolymers were prepared in methylene dichloride (0.1 mg/mL) and spin-cast on graphite in order to observe individual macromolecules. Figure 2 shows the AFM images of comblike block copolymers, PCEVE$_{230}$-*g*-(PS$_{106}$-*b*-PI$_{21}$) (a) and PCEVE$_{230}$-*g*-(PS$_{106}$-*b*-P*I*$_{115}$) (b,c). They reveal individual molecules lying flat on the substrate. In all cases, these macromolecules appear as uniform object, which adopt an ovoid conformation. Their homogeneity in size confirms the data obtained from SEC.

The topographic analysis of the PCEVE$_{230}$-*g*-(PS$_{106}$-*b*-PI$_{21}$) (2), Figure 2a, indicates for the macromolecules an average contour length of about 58 nm and a width of 30 nm, whereas their height is only 1.5 nm, indicating that they are completely flattened on the substrate due to the good affinity of PI and PS blocks with the substrate. For the PCEVE$_{230}$-*g*-(PS$_{106}$-*b*-P*I*$_{115}$) (3) having the same backbone and polystyrene block DP$_n$s as (2) and a much longer external polyisoprene block, the average contour length (about 65 nm) and the width (35 nm) are slightly larger than that of the previous sample, in agreement with the larger volume occupied by the PI blocks. The height is again only 1.5 nm. The phase image of PCEVE$_{230}$-*g*-(PS$_{106}$-*b*-P*I*$_{115}$), Figure 2c, shows clearly the formation of separated polystyrene and polyisoprene domains corresponding to a core−shell type morphology, the white external corona corresponding to soft polyisoprene blocks and the darker internal domain related to the hard polystyrene segments attached to the central backbone. Because of the much shorter polyisoprene blocks, it was not possible to observe the phase separation on the phase image of PCEVE$_{230}$-*g*-(PS$_{106}$-*b*-PI$_{21}$).

4.2. Solution Properties. The solution properties of F−PS combs and of PS-*b*-PI comb block copolymers were investigated using static and dynamic light scattering in THF, a common good solvent for the PCEVE backbone, the polystyrene, and the polyisoprene blocks.

Figure 3 shows the typical normalized autocorrelation functions for the F−PS comb (1) and the PS-*b*-PI comb (3) at $T =$ 25 °C. The CONTIN analysis of the autocorrelation functions shows a monomodal decay time distribution at all scattering angles. A typical result is illustrated in Figure 3 and shows for the two samples very narrow size distribution. This confirms the presence in solution of a single comblike particle corresponding to isolated macromolecules with very low polydispersity, as confirmed by SEC and observed by AFM. The corresponding apparent hydrodynamic radii were calculated according to Stokes−Einstein relation, under the assumption that the scattering particles behave as hard spheres. Even though the macromolecules are of very high molar mass, their hydrodynamic radius is very small and ranges from 20 to 30 nm, in agreement with a very compact structure of the polymer architecture. The corresponding hydrodynamic radii are collected in Table 2.

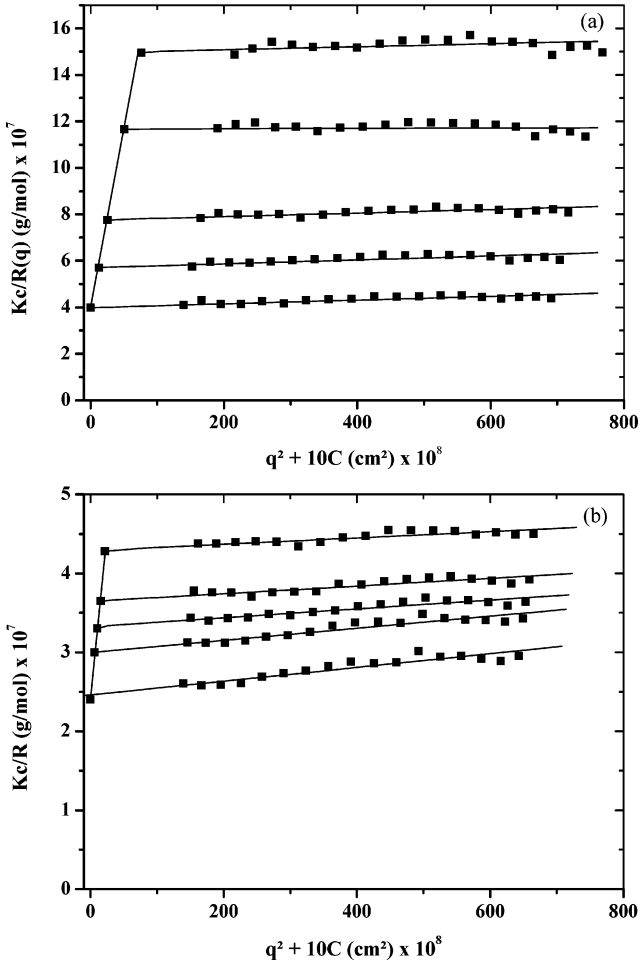

Figure 4. Zimm diagrams for: (a) PCEVE$_{230}$-*g*-PS$_{106}$−F, (b) PCEVE$_{230}$-*g*-(PS$_{106}$-*b*-PI$_{115}$), obtained in THF at 25 °C.

The radius of gyration of the isolated combs was measured by static light scattering (SLS) in THF. Figure 4 shows the Zimm plots obtained for the PCEVE$_{230}$-*g*-PS$_{106}$−F (1), and PCEVE$_{230}$-*g*-(PS$_{106}$-*b*-P*I*$_{115}$) (3) combs. The radii of gyration and the hydrodynamic radii are collected in Table 2. The ratio R_g/R_{H0} ranges from 1.05 to 1.27. This ratio R_g/R_{H0} is more important for the PCEVE-*g*-PS−F than for the PCEVE-*g*-(PS-*b*-PI) and decreases with the length of the branches, in agreement with the morphology of the object. PCEVE-*g*-(PS−F) is included between a sphere and a wormlike conformation, while PCEVE-*g*-(PS-*b*-PI) is close to a sphere conformation. Hydrodynamic radii and radii of gyration were also calculated from the prolate ellipsoid model, assuming that the values of the main and minor axis satisfy a planar zigzag backbone and Gaussian branched chains.[23] The model needs only two parameter values of the semimajor and the semiminor axes, *a* and *b*, for

calculation of the translational diffusion coefficient D_0 to be compared with experimental values.

Hydrodynamic radii were calculated using the prolate ellipsoid model, where the values of the semimajor and the semiminor axes a and b are assumed to have a planar zigzag backbone and Gaussian branched chains, respectively. The translational diffusion coefficient D_0 can be written as:

$$D_0 = k_B T/6\pi\eta_0 a G(\rho) \quad (1)$$

$$G(\rho) = (1-\rho^2)^{1/2}/\ln[(1+(1-\rho^2)^{1/2})/\rho] \quad (2)$$

where η_0 is the solvent viscosity, $\rho = b/a$ is the axial ratio, and $k_B T$ the Boltzman energy.[23]

Radius of gyration was calculated from the relation:

$$R_g = a[(1+2\rho^2)/3]^{1/2} \quad (3)$$

The PCEVE backbone chain is assumed to have a planar zigzag conformation, while the PS-*b*-PI branch is the Gaussian coil. Within this model, the dimensions of the ellipsoid can be estimated according to: $2a = L_{PCEVE} + 2\langle L_{PS}^2\rangle^{1/2} + 2\langle L_{PI}^2\rangle^{1/2}$ and $b = \langle L_{PS}^2\rangle^{1/2} + \langle L_{PI}^2\rangle^{1/2}$, where L_{PCEVE} is given in eq 4, and the root-mean-square end-to-end distance of linear PS and PI for $\langle L_{PS}^2\rangle^{1/2}$ and $\langle L_{PI}^2\rangle^{1/2}$ is given in eqs 5 and 6.

$$L_{PCEVE} = 0.252\ DP_{PCEVE}\ \text{nm} \quad (4)$$

$$\langle L_{PS}^2\rangle^{1/2} = 7.00\times10^{-2}\, M_{PS}^{1/2}\ \text{nm} \quad (5)$$

$$\langle L_{PI}^2\rangle^{1/2} = 9.00\times10^{-2}\, M_{PI}^{1/2}\ \text{nm} \quad (6)$$

In this model, we assume that each block (PS and PI) has a Gaussian conformation and evolves independently from each other at the junction point. The calculated results were found to be in very good agreement with the experimental data (Table 2). These results assumed an extended backbone conformation owing to the multibranched structure and a Gaussian branch conformation, as we can see from the AFM images.

Apart from system 2, the R_g/R_{H0} values are in good agreement with theoretical calculation assuming a prolate model. The comparison with AFM experiments lead to a reasonable agreement, and the results are for system (2): (i) AFM ($2a$ = 58 nm, $2b$ = 30 nm), deposited without solvent, and the prolate model gives ($2a$ = 80 nm, $2b$ = 21 nm) in solution. (ii) System (3): AFM ($2a$ = 65 nm, $2b$ = 35 nm), deposited without solvent, and the prolate model gives ($2a$ = 88 nm, $2b$ = 30 nm) in solution.

The influence of the polystyrene chain architecture on the polymer−solvent interaction parameters was investigated by the determination the theta (θ) conditions for F−PS combs. For that purpose, we measured using elastic light scattering the second virial coefficient A_2 both for the comblike PCEVE$_{230}$-*g*-PS$_{106}$−F and for a homopolymer corresponding to the single linear branch, F−PS$_{106}$, in cyclohexane a θ solvent of F−PS. The contribution on A_2 values of the ethyl vinyl ether unit that links each F−PS branch to the backbone in the comb structure, which represents less than 1% in weight of the F−PS, can be neglected. The A_2 values are plotted against T in Figure 5. The temperature at which A_2 is equal to 0 corresponding to θ conditions, is equal to 29 °C for the linear polystyrene F−PS$_{106}$ and 21.5 °C for the PCEVE$_{230}$-*g*-PS$_{106}$−F. The lower value observed for the linear PS, compared to literature data ($\theta_{\text{linear PS}}$ = 34.5 °C), can be explained by the relatively low molar mass of the PS branch. Beside, the much lower θ value found for the F−PS comb (M_n= 2.1×10^6 g/mol) confirms the important role of the chain architecture on the solubility parameters of polystyrene, i.e., the highly branched architecture increases the solvent quality with respect to linear polystyrene. This result is in agreement with data reported by other groups[24−26] and confirms that linear and comb polystyrene do not have the same θ temperature of 34.5 °C, as it was observed.[27]

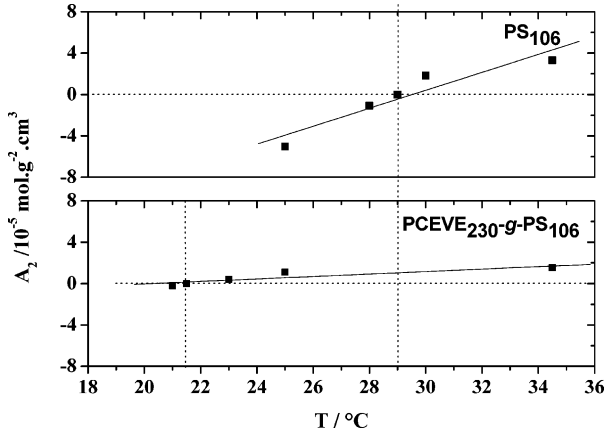

Figure 5. Evolution of A_2 as a function of temperature for a linear F−PS$_{106}$ and the PCEVE$_{230}$-*g*-PS$_{106}$−F comb in cyclohexane. The vertical dashed lines indicate the θ temperature (A_2 = 0) for the two polymers.

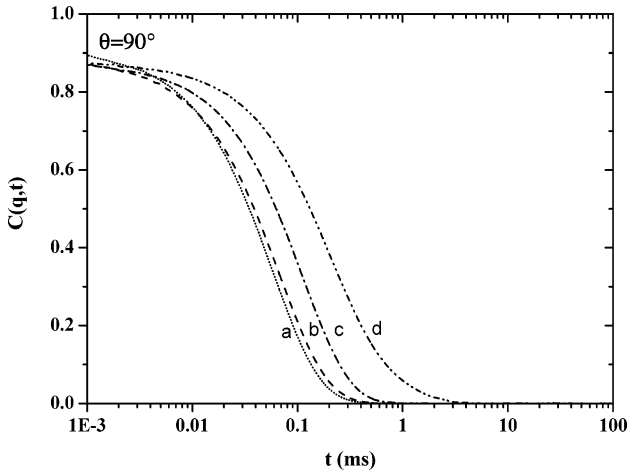

Figure 6. Normalized field correlation for the PCEVE$_{230}$-*g*-(PS$_{106}$-*b*-PI$_{115}$) comb in different solvents (θ = 90°) (a, THF at c = 0.6 g/l; b, heptane at c = 1.7 g/l; c, decane at c = 2.5 g/l) at t = 25 °C; d: cyclohexane (c = 1.9 g/l) at t = 8 °C.

The influence of the solvent quality on PCEVE-*g*-(PS-*b*-PI) comb copolymers was further investigated in heptane, decane, and cyclohexane and DMF. While THF is a good solvent for both linear PS and PI, heptane and decane are good solvents for PI and bad solvents for PS, respectively. Cylohexane is a good solvent for PI and a θ solvent for PS (θ = 21.5 °C for our branched PS). Finally, DMF is a good solvent for PS and a bad solvent for PI.

The solution behavior of PS-*b*-PI comb copolymers of different PI block lengths was investigated using dynamic light scattering. Figure 6 shows typical normalized field correlation functions of comb copolymers PCEVE$_{230}$-*g*-(PS$_{106}$-*b*-PI$_{115}$) in these different solvents. The same results were observed for systems (2) and (2′). In all examined solvents, the CONTIN analysis of the autocorrelation functions shows monoexponential decay time distribution, indicating the presence of a single and distinct distribution of objects, corresponding to isolated comb molecules. Data indicate the absence of any detectable aggregation. The evolution of the hydrodynamic radius versus

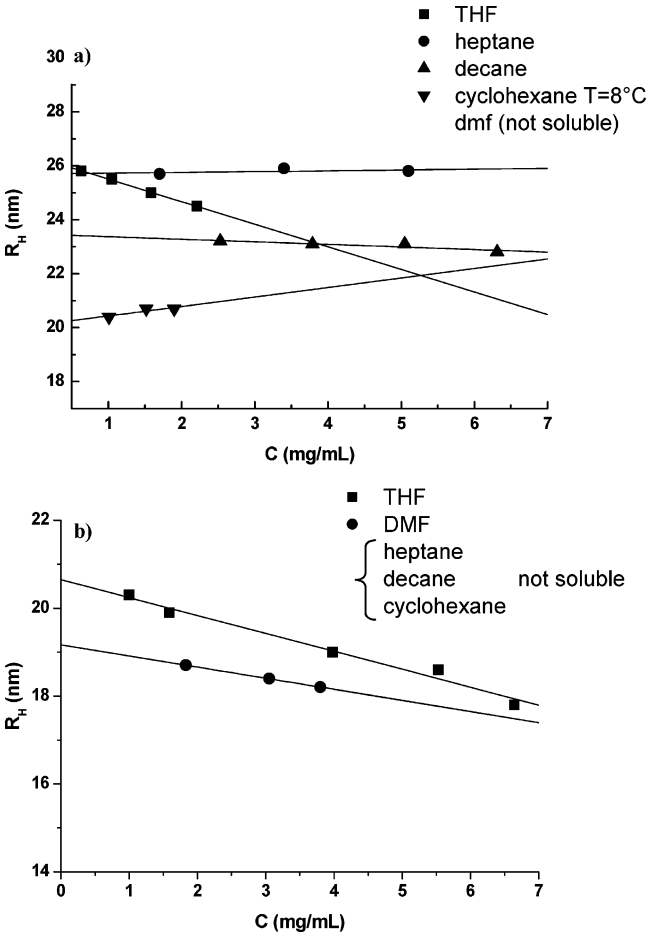

Figure 7. Evolution of the hydrodynamic radius at 25 °C in different solvents for: (a) $PCEVE_{230}$-*g*-(PS_{106}-*b*-PI_{115}) with long polyisoprene blocks; (b) $PCEVE_{230}$-*g*-(PS_{106}-*b*-PI_{21}) with short polyisoprene blocks.

Table 3. Hydrodynamic Radius of $PCEVE_{230}$-*g*-(PS_{106}-*b*-PI_{115}) in Different Solvents at 25 °C

solvent	R_{H0} (nm)
THF	26.3
heptane	25.7
decane	23.5
cyclohexane ($T = 8$°C)	20.2

the $PCEVE_{230}$-*g*-(PS_{106}-*b*-PI_{115}) concentration is presented in Figure 7a for different solvents. The slope observed for THF is in agreement with the behavior in a good solvent (virial dynamic coefficient is indeed $k_d > 0$), whereas all hydrocarbons behave as a bad solvent for the PS in the comblike polymers. In THF, the PI corona and the PS core tends to adopt a more extended conformation. In the case of heptane and decane at 25 °C and in cyclohexane at 8 °C (a temperature below the θ temperature of the PS branches), the hydrodynamic radius of the diblock comb (Table 3) becomes smaller and decreases in the order heptane > decane > cyclohexane, $T = 8$ °C, due to contraction of the PS core, which tends to collapse, but the macromolecules still remain as isolated objects thanks to the corona formed by the PI blocks. The reduction in the hydrodynamic radius from THF to cyclohexane at 8 °C corresponds to a 121% decrease of the hydrodynamic volume of the macromolecule. It is worth noting that comb copolymers remain as isolated molecules and only undergo dimensional changes with the solvent quality and/or the temperature. A very different behavior is observed for the corresponding linear PS-*b*-PI diblocks, which behave either as unimeric molecules or self-organize into micelles depending on the solvent quality. In DMF, both the diblock PS-*b*-PI (2′) and (3) systems are insoluble due to the direct interaction of the outer PI blocks with DMF, a bad solvent of PI. A different situation is observed in the case of system (2) (Figure 7b), which remains soluble and forms isolated unimolecular objects without any detectable aggregation. It is believed that the very short polyisoprene's blocks are not able to shield the polystyrene core, allowing DMF molecules to penetrate inside the PS core.

The effect of temperature on the molecular dimensions and organization of the F−PS and diblock PS-*b*-PI combs has been investigated in cyclohexane below and above the PS temperature θ in the range of 8−55 °C. Values of the hydrodynamic radii are collected in Table 4. A decrease in the temperature leads to a decrease of the hydrodynamic radius for all of the examined samples. The hydrodynamic radius of the F−PS comb system (1) decreases continuously from 55 to 25 °C, then the F−PS comb precipitates. This result is related to the fact that cyclohexane is a bad solvent for polystyrene at temperatures lower that the θ temperature, i.e., 21.5 °C. For diblock combs (2) and (3) systems, the hydrodynamic radius also decreases significantly with temperature. The comb copolymer with the smaller PI block (2) starts to precipitate at 15 °C, whereas the presence of longer PI blocks for system (3) forms a protective PI shell that avoid precipitation, even at the lowest investigated temperature. When decreasing the temperature, the PS blocks tend to shrink; this result again in a significant reduction of the size of the PS core and therefore the whole macromolecule, as illustrated in Scheme 2. When the protecting role of the PI shell

Table 4. Evolution of the R_{H0} with the Temperature for Different Comblike Diblock Copolymers $PCEVE_{230}$-*g*-(PS_x-*b*-PI_y) in Cyclohexane

ref no.	constitutive blocks $\overline{DP}_n$ PCEVE-PS−PI	R_{H0} $T = 55$ °C (nm)	R_{H0} $T = 45$ °C (nm)	R_{H0} $T = 35$ °C (nm)	R_{H0} $T = 25$ °C (nm)	R_{H0} $T = 15$ °C (nm)	R_{H0} $T = 8$ °C (nm)
(1)	230−106−0	16.4	16.0	15.8	15.2	precipitated	precipitated
(2)	230−106−21	19.3	18.8	18.5	17.7	beginning of precipitation	beginning of precipitation
(3)	230−106−115	25.0	24.5	23.5	23.2		20.2

Scheme 2. Contraction/Extension Process of the Polystyrene Core with Variation of the Temperature for PS-*b*-PI Comb Block Copolymers in Cyclohexane

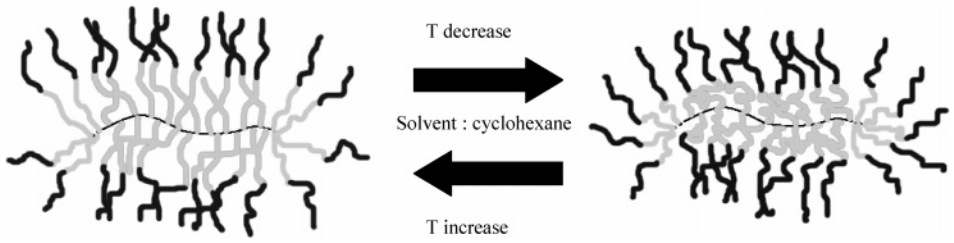

is efficient, the important volume variation, close to 90%, observed between 55 and 8 °C, is fully reversible, resulting in the formation of reversibly thermosensitive nano-objects.

5. Conclusion

The synthesis of PCEVE-*g*-PS−F comblike polymers and PCEVE-*g*-(PS-*b*-PI) core−shell-like copolymers with controlled chain parameters was successfully achieved by the grafting onto approach. AFM and light scattering experiments were used to highlight their properties in solution and solid states. AFM experiments show that the molecular brushes adsorbed on graphite have an ovoid conformation with distinctable PS core and PI shell domains. These comblike diblock copolymers are in solution as isolated unimolecular object that can be "seen" as a unimolecular micelle in a selective solvent for the outer block. These nanoparticles, and aggregates-free, are much more stable than micelles formed by the self-assembly of linear diblocks. They present also an interesting reversible capacity to respond to the environment and the temperature with an important extension/contraction of their volume. These characteristics could make them useful, particularly as thermosensor nanoparticles.

References and Notes

(1) Desvergne, S.; Heroguez, V.; Gnanou, Y.; Borsali, R. *Macromolecules* **2005**, *38*, 2400−2409.
(2) Zhang, B.; Zhang, S.; Okrasa, L.; Pakula, T.; Stephan, T.; Schmidt, M. *Polymer* **2004**, *45*, 4009−4015.
(3) Viville, P.; Leclere, P.; Deffieux, A.; Schappacher, M.; Bernard, J.; Borsali, R.; Bredas, J.-L.; Lazzaroni, R. *Polymer* **2004**, *45*, 1833−1843.
(4) Liu, Y.; Abetz, V.; Mueller, A. H. E. *Macromolecules* **2003**, *36*, 7894−7898.
(5) Qin, S.; Matyjaszewski, K.; Xu, H.; Sheiko, S. S. *Macromolecules* **2003**, *36*, 605−612.
(6) Mijovic, J.; Sun, M.; Pejanovic, S.; Mays, J. W. *Macromolecules* **2003**, *36*, 7640−7651.
(7) Zhang, M.; Breiner, T.; Mori, H.; Muller, A. H. E. *Polymer* **2003**, *44*, 1449−1458.
(8) Kjoniksen, A.-L.; Nystrom, B.; Tenhu, H. *Colloids Surf., A* **2003**, *228*, 75−83.
(9) Francis, M. F.; Piredda, M.; Winnik, F. M. *J. Controlled Release* **2003**, *93*, 59−68.
(10) Bailly, C.; Stephenne, V.; Muchtar, Z.; Schappacher, M.; Deffieux, A. *J. Rheol.* **2003**, *47*, 821−827.
(11) Zhang, M.; Drechsler, M.; Mueller, A. H. E. *Chem. Mater.* **2004**, *16*, 537−543.
(12) Zhang, J. X.; Qiu, L. Y.; Zhu, K. J.; Jin, Y. *Macromol. Rapid Commun.* **2004**, *25*, 1563−1567.
(13) Ishizu, K.; Tsubaki, K.; Uchida, S. *Macromolecules* **2002**, *35*, 10193−10197.
(14) Deffieux, A.; Schappacher, M. *Macromolecules* **1999**, *32*, 1797−1802.
(15) Schappacher, M.; Billaud, C.; Paulo, C.; Deffieux, A. *Macromol. Chem. Phys.* **1999**, *200*, 2377−2386.
(16) Siegert, A. J. F. *MIT Rad. Lab. Rep.* **1943**, no. 465.
(17) Cheng, G.; Boeker, A.; Zhang, M.; Krausch, G.; Mueller, A. H. E. *Macromolecules* **2001**, *34*, 6883−6888.
(18) Qin, S.; Matyjaszewski, K.; Xu, H.; Sheiko, S. S. *Macromolecules* **2003**, *36*, 605−612.
(19) Neugebauer, D.; Zhang, Y.; Pakula, T.; Sheiko, S. S.; Matyjaszewski, K. *Macromolecules* **2003**, *36*, 6746−6755.
(20) Ryu, S. W.; Hirao, A. *Macromolecules* **2000**, *33*, 4765−4771.
(21) Schappacher, M.; Deffieux, A. *Macromolecules* **2000**, *33*, 7371−7377.
(22) Muchtar, Z.; Schappacher, M.; Deffieux, A. *Macromolecules* **2001**, *34*, 7595−7600.
(23) Nemoto, N.; Nagai, M.; Koike, A.; Okada, S. *Macromolecules* **1995**, *28*, 3854−3859.
(24) Roovers, J. E. L. *Polymer* **1975**, *16*, 827−832.
(25) Franta, E.; Candau, F. *Makromol. Chem.* **1971**, *149*, 41−50.
(26) Decker, D. *Makromol. Chem.* **1969**, *125*, 136−160.
(27) Terao, K.; Nakamura, Y.; Norisuye, T. *Macromolecules* **1999**, *32*, 711−716.

MA061169L